THE ARCHIVE OF MECHANICAL ENGINEERING

Vol. LI 2004 Number 2

Key words: *car steering system, friction, resistance torque, self-returnability, rig study*

JÓZEF KNAPCZYK), MICHAŁ MANIOWSKI**)*

EXPERIMENTAL RIG STUDY ON RESISTANCE FORCES IN CAR STEERING SYSTEM WITH RACK AND PINION

The authors present the results of experimental rig study on resistance forces in a rack and pinion steering system without power assistance of a small car with MacPherson front suspension. The influence of a harmonic steering angle excitation, with frequency ranging from 1 to 3 Hz, and different wheel load conditions on self-returnability, sensitivity, and friction forces in the steering system is studied. These characteristics are responsible for the car directional stability at high-speed of cruising or during braking maneuver, and influence comfort, effort, and good feeling of the car driver. On the basis of experimental results, some parameters (equivalent moment of friction forces and stiffness coefficients) of a simplified model are estimated for different excitations and load conditions.

NOMENCLATURE

Reference frames:

W – ($OXYZ$) fixed to the car body,

W_b – ($0_b x_b y_b z_b$) fixed to the wheel knuckle,

W_p – ($0_p x_p y_p z_p$) fixed to the center of tire contact patch.

Points:

A_i – center of the joint linking the i-th (i = 1, 2, 3) rod with the car body [mm],

B_i – center of the joint linking the i-th (i = 1, 2...4) rod with the wheel knuckle [mm],

*) *Institute of Automobiles and Internal Combustion Engines, Cracov University of Technology, Al. Jana Pawła II 37, 31-864, Poland; E-mail: J_kn@pobox.mech.pk.edu.pl.*

**) *Institute of Automobiles and Internal Combustion Engines, Cracov University of Technology, Al. Jana Pawła II 37, 31-864, Poland; E-mail: mmaniowski@poczta.onet.pl.*

B_4 – wheel center [mm],
P – center of the tire contact patch of the free rotating wheel [mm].
Tensors:
$\mathbf{a}_i$ – position vector of the point A_i described in the assigned reference frame [mm],
$\mathbf{b}_i$ – position vector of the point B_i described in the assigned reference frame [mm],
$\mathbf{u}_{ka}$ – unit vector of the kingpin axis,
$\mathbf{u}_s$ – unit vector of the main spring axis,
$\mathbf{e}_1$ – unit vector of the revolute joint axis at the lower wishbone.
Suspension and steering system geometry:
d_i – i-th rod length (i = 1, 3) [mm],
s – main spring deflection from the suspension design position [mm],
p – steering rack displacement relative to its housing [mm],
δ_w – road wheel steer angle [deg],
δ_h – hand wheel steering angle [deg],
δ_p – angular displacement of the pinion [deg],
r_τ – caster offset [mm],
r_s – kingpin offset at the ground (brake/roll radius) [mm],
r_p – arm of the wheel normal force [mm].
Forces and moments:
F_{zw} – wheel normal force (left or right) [N],
F_r – axial force in the tie rod (left or right) [N],
F_{sr} – axial force in the steering rack [N],
M_h – steering wheel torque [Nm],
$T_{h,e}$ – torque of friction forces reduced to the steering shaft [Nm].
Coefficients:
c_{ss} – torsional stiffness coefficient of the steering shaft [Nm/rad],
c_{ka} – torsional stiffness coefficient (stabilization coefficient) reduced to kingpin axis [Nm/rad],
$c_{h,e}$ – torsional stiffness coefficient (stabilization coefficient) reduced to the handwheel [Nm/rad].

1. Introduction

The highest resistance forces in a car steering system occur when the wheels are turned with the stationary car. The maximum steering torque in a moving vehicle is about one third of the static torque [4]. The steering hand-wheel torque needed to move the road wheels slowly against various form of resistance, at zero or very low vehicle speeds, is an important parameter in the design of a car steering system. It influences the fundamental decisions about the choice of stationary gear ratio, whether or not power assistance is necessary, and the nature of such a power assistance, still taking into account other geometrical constraints, such as the limit on bump steer and maximal steer angles.

Recently, much effort has been put in tuning the car steering system to obtain a good driver feeling concerning car comfort, responsiveness, and straight line stability at high speeds of cruising. These characteristics strongly influence driver's subjective evaluation of the vehicle [5], [6]. The amount of tactile feedback to the driver through the hand-wheel can be controlled. Specifically, the hand-wheel restoring torque provides information to the driver regarding road condition and vehicle maneuverability. The amount of restoring torque is a function of chassis design, mainly its geometry, and friction dependent transmissibility of wheel loads back to the hand-wheel.

The torque at the steering wheel necessary to drive a car along some desired trajectory is a function of several forces [1]:

a) Conservative forces, caused by a stabilization moment of a suspension, self-aligning torque of the tire, and elastic deflections forces in elements like main spring, elastomeric bushes, or anti-roll bar loaded by the steering wheel angular displacement.
b) Dissipative forces, associated with friction in the joints, including dampers and suspension links, rubber bushes, and strut sliders. Loads in the joints are affected by any change of wheel load, especially the cornering forces. In order to minimize sliding friction at suspension joints, it is now normal to use a cylindrical rubber/elastomeric bush that distorts in shear as the suspension operates, so most of suspensions have elements of rubber type friction and stiffness. Rubber bushes are some practical compromise with low cost, low maintenance and good vibration isolation.
c) Inertial forces and gyroscope moments responsible for the system response to dynamic excitations, like for example, during crossing a discrete obstacle on the road.

The share of particular forces in total steering resistance force changes according to car speed, lateral acceleration, and external load acting on a steering system, frequency of excitation and wear state of joint elements.

The effect of conservative forces can be described by a relation of the steering wheel torque versus its angular displacement. The typical characteristic of the steering torque, that driver exerts at the hand-wheel, as a function of the steering angle, is shown in Fig. 1 for a car taking a slalom maneuver with constant speed [5]. If the loading conditions of a steering system are constant and the excitation amplitude is small, then this relation is quasi-linear and can be described by using a stabilization coefficient of steering system [1], [5]. The self-returnability of the steering system can be achieved when the stabilization coefficient is positive.

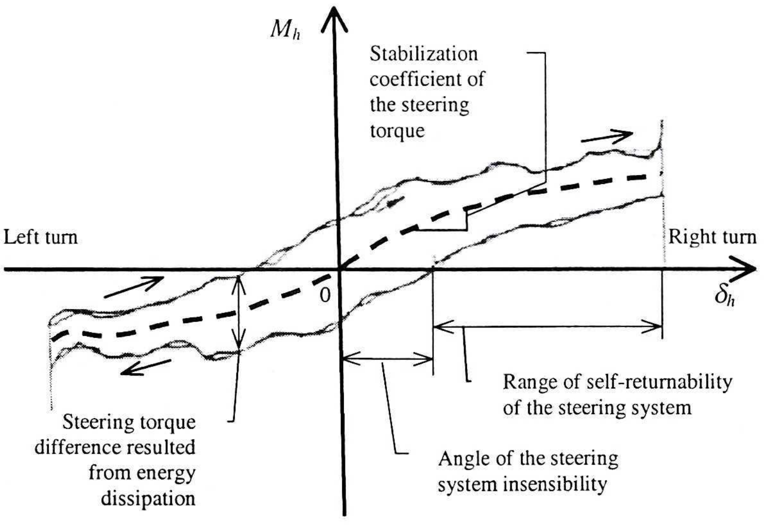

Fig. 1. Typical characteristics of the steering torque (measured at the hand-wheel) as a function of the steering angle for a car taking a slalom maneuver with a constant speed [5]

The dissipative forces are described by a typical hysteresis loop noticed on the steering torque characteristics in Fig. 1 [3]. The area of hysteresis loop is proportional to the quantum of energy used by the driver to make a desired maneuver. The width of hysteresis loop can be used to describe the insensitivity coefficient of steering system [5], [6], and the angle of steering system insensitivity, Fig. 1, where the system self-return properties are not achieved although the stabilization coefficient is greater than zero.

It is desirable for the forward efficiency of the steering system to be high, in order to keep the hand-wheel resistant torque low. On the other hand, a low reverse efficiency helps to reduce the transmission of road roughness disturbances back to the driver, at the expense of the driver less sensation, what deteriorates his/her possibility to estimate frictional state of the road.

The proper choice of the stabilization and insensitivity coefficients for a steering system results from a compromise between contradictory requirements [3], [4]. A satisfying comfort level is assured by increased friction in the steering system (diminished vibration transmission to the steering wheel) and smaller stabilization coefficient (smaller driving forces at the steering wheel). However, under these conditions the driver has worse possibility to evaluate current road conditions, what decreases the car active safety.

The design of vehicles having optimal straight line stability requires accurate experimental and simulation results of the steering system response to a small steering wheel angle input, applied for example in pseudo-harmonic manner at frequencies up to a few Hz. This input has an amplitude of about 15 degrees and corresponds to low-g maneuvers at higher speed of cruising. Under these operation conditions, characterized by small changes of the tires' lateral and vertical forces relative to straight ahead conditions, the resistance torque at the handwheel is a consequence primarily of the wheel vertical forces and friction forces in joints of the steering mechanism.

2. Goal and scope of the study

The purpose of this work is an experimental and theoretical study on resistance forces in a small car suspension-steering system, schematically shown in Fig. 2, caused by the steering wheel angular displacements of a sinusoidal manner with small amplitudes, different frequencies (up to 3Hz), and various load conditions.

Main focus of the analysis is concentrated on such characteristics of the suspension-steering system as stabilization and insensitivity coefficients, important in aspects of driver feeling, comfort, and car high-speed directional stability. In-door experiments were carried out only, using a specialized test rig with the car front wheels supported on rotational plates, Fig. 2. This arrangement allowed us to separate the influence of tire characteristics. Under these conditions, the steering system is primarily loaded by the wheel vertical forces, steering wheel torque, with the joints' friction forces and the system inertial forces taken into account.

At the first stage, a model of the considered mechanism is presented, which describes kinematic and load transmission relations in a full range of the road wheels turning and bounce displacements. A simplified model is formulated next, reflecting the system characteristics that are the most important under the operational conditions assumed in this paper. The introduced models are useful in proper designing of the experiment and in understanding the presented results.

Main assumptions taken in the experimental analysis and in formulation of the mechanism models are the following:

- the rack and pinion steering system is of constant gear ratio, without any power assistance,
- the front suspension is without antiroll bar (it has no effect on the stabilizing moment),
- small changes of the wheel steer angle do not cause the suspension bounce motion,

- influence of the tire and the car body movements is separated,
- only technically dry friction appears in the system,
- modules of friction forces are not dependent on the displacement sense in relative motions of joints' elements,
- stiction coefficient is indistinguishable from sliding coefficient,
- the system fundamental natural frequency is over 10 Hz,
- joints are without backlashes,
- mean values and confidence bounds (for 95% level) for all estimates of the formulated model parameters are determined on the basis of the repeated measurement trials.

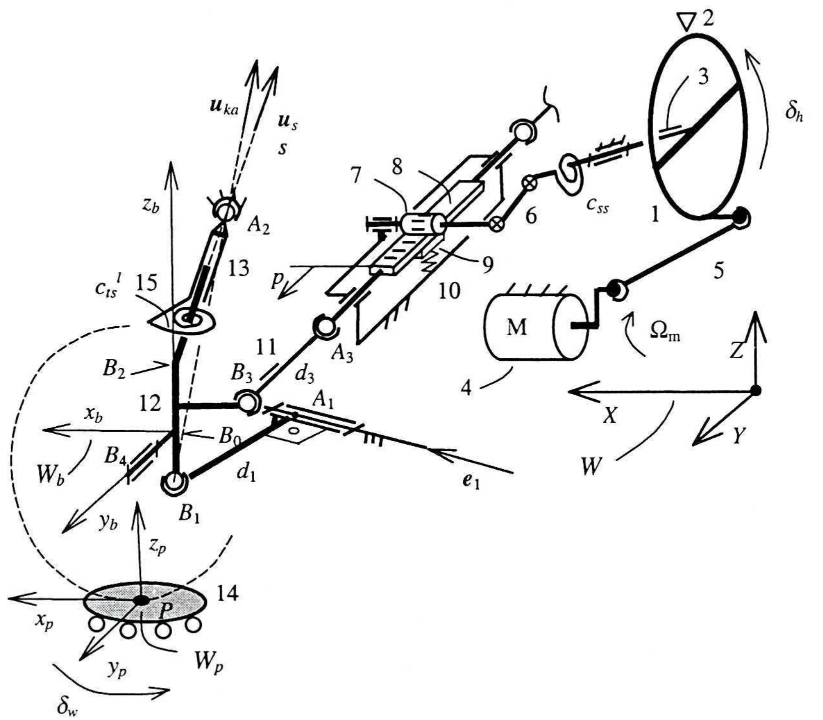

Fig. 2. Kinematic scheme of the front strut suspension with rack-and-pinion steering system in trailing configuration, and road wheels supported on rotational plates of the test stand. Left side is shown only

3. Test rig description

The test rig, depicted in Fig. 2, is composed of the following elements: 1 – steering wheel, 2 – steering angle transducer, 3 – torque transducer at the steering shaft based on strain gauges, 4 – DC-motor fixed to the car body, 5 – coupler linked with the DC-motor crank and with the steering wheel, forming a spatial four-bar linkage, 6 – steering shaft with two universal joints, 7 – pinion, 8 – steering rack, 9 – preloaded yoke, 10 – steering gear housing, d_3 – tie rod, 11 – strain gauges for measurement of axial force in the rod, 12 – wheel knuckle, 13 – strut column with a spring-damper unit, d_1 – lower wishbone, 14 – wheel rotating plates with axial ball bearing of small resistance, 15 – additional torsional spring.

The idea of measurements consists in excitation of an angular displacement of the steering wheel in harmonic fashion by using the spatial four-bar linkage propelled by DC-motor (Fig. 2), having the car body fixed to the stand base under the selected load conditions, and with the front wheels supported on the rotating plates. Taking the advantage of the described linkage, one can obtain a pseudo-sinusoidal excitation with constant amplitude and linearly varying frequency in the range of 0.1 to 3.0 Hz. Measurements of the torque at the steering shaft (3 in Fig. 2) and axial forces in the tie rods (11 in Fig. 2) make it possible to distinguish different friction sources in the mechanism.

An additional torsional spring (15 in Fig. 2), with a known stiffness constant c_{ts} = 6.5 Nm/deg, mounted along axis of spring-damper column, was used during measurements in order to increase the stabilization moment relative to the kingpin axis, what simulates an action of the tire side force and self-aligning torque.

Two gyroscopic transducers were used to measure the angular velocity of the steering wheel (steering angle rate) and angular velocity of the wheel knuckle with respect to Z-axis (steer angle rate). A set of three mono-axis accelerometers was utilized to estimate the acceleration state of the wheel knuckle. The 16-bit analog-to-digital converter and laptop-type PC were used for acquisition and visualization of the experimental results. The 20 Hz sampling frequency was chosen for measurements for the static excitation and 200 Hz for a dynamic one.

In order to estimate the influence of different factors on the steering system resistance forces, the performed experimental trials are categorized with respect to the excitation type of the steering wheel angular movements, as:

stat – quasi-static sinusoidal excitation with frequency below 0.1 Hz,

dyn – sinusoidal excitation with frequency in the range of 1.0 to 3.0 Hz,

and the type of load conditions in the steering-suspension system:

A. front wheels supported at rotating plates, suspension in the design position,
B. front wheels supported at rotating plates, normal load increased relatively to the design position by 1.5 kN at the front axle,
C. front wheels supported at rotating plates, suspension in the design position, an additional torsional spring (Fig.2–15) attached to the kingpin axis of both front wheels,
D. front wheels over the ground.

4. Models of the suspension-steering system

In this section, we formulate the mechanism model that makes it possible to better understand the relations between the motion and resistant loads in a full range of the suspension bounce displacements and the steer angles of road wheels.

The scheme of the model suitable for the analysis of the considered problem is presented in Fig. 2. The suspension bounce motion is described by coordinate s – deflection of the main spring along its axis, denoted by u_s. The coordinate s varies in the range of [−120, 80] mm with respect to the suspension design position. The steering rack displacement, denoted by p, ranges from [−80, 80] mm.

Three reference systems are distinguished in Fig. 2:

- $\{W\}$ the car body reference system with XZ-plane coinciding with the car longitudinal plane of symmetry;
- $\{W_b\}$ the wheel knuckle reference frame with origin at point B_0, with y-axis coinciding with the wheel spin axis, where z-axis points upward and passes through point B_1,
- $\{W_p\}$ the tire reference frame with origin at the center of tire contact patch P, xy-plane coincident with the ground plane, y_p-axis is a normal projection of y_b onto the ground plane.

Kinematic constraint equations, developed for the considered mechanism, are solved in a closed form with respect to the knuckle position and orientation as functions of s and p by using the vector method described in [2].

Geometrical parameters of the model presented in Fig. 2, estimated on the basis of the mechanism technical drawings, are given below for the design position. The front suspension in the design position is under normal load F_{zw} = 2.50 kN per wheel, what corresponds to s = 0, and with steering system set for the car running straight ahead, what means $p = 0$ (wheel toe and camber angles equal to zero).

The linear dimensions are given in mm (superscript T denotes a vector transposition):
$\mathbf{a}_1 = [2.5\ \ 315.0\ \ -74.0]^T$, $\mathbf{a}_2 = [-17.0\ \ 502.0\ \ 523.0]^T$, $\mathbf{a}_3 = [-92.0\ \ 197.0\ \ 142.0]^T$, $\mathbf{b}_0 = [0.0\ \ 603.0\ \ 0.0]^T$, $\mathbf{b}_1 = [2.5\ \ 603.0\ \ -104.0]^T$, $\mathbf{b}_2 = [-12.6\ \ 540.0\ \ 318.5]^T$, $\mathbf{b}_3 = [-132.0\ \ 538.0\ \ 147.0]^T$, $\mathbf{b}_4 = [0.0\ \ 635.0\ \ 0.0]^T$, $r_w = 269$, $d_1 = 290.0$ $d_3 = 343.4$.
Unit vectors: $\mathbf{e}_1 = [1\ 0\ 0]^T$, $\boldsymbol{u}_s = [-0.0211\ -0.1827\ 0.9830]^T$, $\boldsymbol{u}_{ka} = [-0.0307\ -0.1590\ 0.9868]^T$ (this orientation of the kingpin axis corresponds to kingpin inclination angle $\sigma = 9.15$ deg, and castor angle $\tau = 1.78$ deg). The model kinematic characteristics have been verified experimentally.

The basic characteristic of the analyzed steering system relates the changes of steer angles of both wheels with the steering rack displacement

p (Fig. 3a), which in turn is a function of steering wheel angle (Fig. 3b). The presented relationship, where the difference of steer angles between left and right wheels grows for larger steering angles, is typical for a steering linkage [1] and can be described by an instantaneous kinematic ratio for given values of s and p in the following way:

$$i_{hw} = \frac{\partial \delta_h}{\partial \delta_w} \quad \text{(different for a left and right road wheel)} \tag{1}$$

The overall ratio of the steering system, expressed by (1), can be considered as a consequence of two factors. The first is associated with motion transmission from the steering wheel to the rack displacement, Fig. 3b, described by a proper ratio:

$$i_{hp} = \frac{\partial \delta_h}{\partial p} \tag{2}$$

The second takes into account the steering linkage relations transforming the rack displacement into a left or right wheel, Fig. 3a, expressed as follows:

$$i_{pw} = \frac{\partial p}{\partial \delta_w} \quad \text{(different for a left and right road wheel)} \tag{3}$$

Thus, the equations (1), (2) and (3) obey:

$$i_{hw} = i_{hp}\, i_{pw} \tag{4}$$

For the considered steering system, the ratio (2) is constant and only the ratio (3) is responsible for the changes of the overall ratio (4), that reach about 30% at extreme positions of the steering linkage, Fig.5b.

For an analysis in a close vicinity of some operation point chosen by a selection of s and p, the introduced kinematic ratios can be assumed constant. The steering system considered in the paper is characterized in the design position by the following ratios:

$$i_{hw} = 21.8 \text{ [rad/rad]}, \; i_{hp} = -167 \text{ [rad/m]}, \; i_{pw} = -0.1305 \text{ [m/rad]}.$$

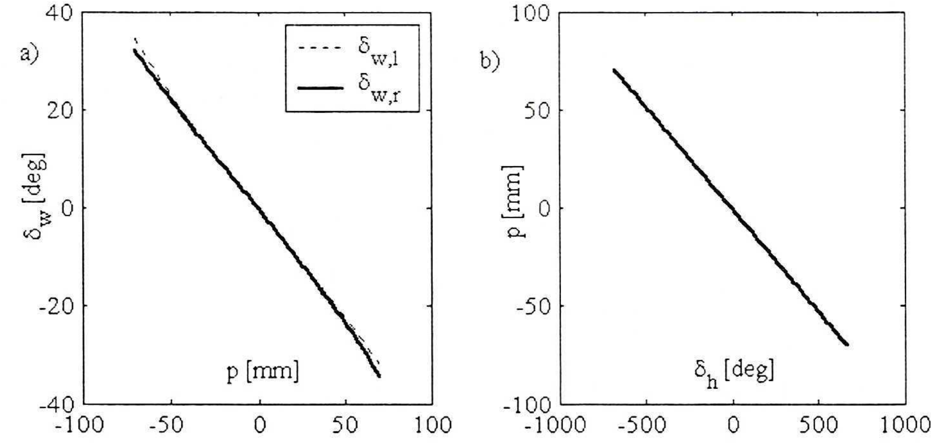

Fig. 3. a) Steer angles of the road wheels $\delta_{w,l}$ and $\delta_{w,r}$ (left and right) versus the steering rack displacement p; b) p versus steering angle δ_h. Suspension is in the design position

External load acting on the steering system in the tire contact patch can be described by a vector:

$$F^p = [F_x^p \ \ F_y^p \ \ F_z^p \ \ M_x^p \ \ M_y^p \ \ M_z^p]^T \tag{5}$$

where the six components in brackets are: forces – longitudinal, lateral, and vertical; torques – overturning, rolling resistance and aligning, respectively.

These components of the tire load can be reduced to the knuckle kingpin axis for a particular position of the suspension-steering system in the following way. First, a scalar value of the torque M_z vertical to the ground plane is determined by:

$$M_z = [r_s \ \ r_\tau \ \ r_p][F_x^p \ \ F_y^p \ \ F_z^p]^T + M_z^p \tag{6}$$

where: r_s is roll radius, r_τ – castor offset, and r_p – arm of the wheel normal force [1]. These geometrical parameters describe the position and orientation of the kingpin axis with respect to the center of tire contact patch. The introduced parameters are dependent on the suspension vertical position and wheel steer angle, what is presented in Fig. 4. The roll radius r_s, positive in this design, is approximately constant. The castor offset r_τ changes significantly in magnitude and sign. It ranges from – 55 mm for the wheel outer in a curve turned in extreme position, to +88 mm for the wheel inner in a curve turned in a corresponding extreme position. The third parameter r_p represents some fictitious arm on which the tire normal force acts yielding the component of the torque M_z loading the wheel knuckle. The introduced parameters play a significant role in the design of a car suspension-steering system. A method of their determination is given in [1].

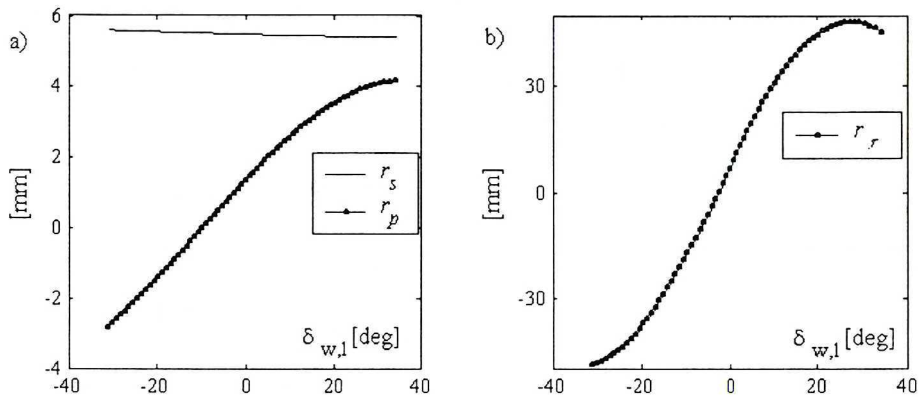

Fig. 4. Variation of: r_s – roll radius, r_p – arm of the wheel normal force (a), and r_τ – castor offset (b) versus road wheel steer angles for a left wheel. Suspension is in the design position

The magnitude of torque relative to the kingpin axis for a given position can be determined by:

$$M_{ka} = [M_x^p \;\; M_y^p \;\; M_z]\, \boldsymbol{u}_{ka} \tag{7}$$

where: M_z is described by (6) and $\boldsymbol{u}_{ka} = [u_x \;\; u_y \;\; u_z]^{\mathrm{T}}$ is a unit vector of the kingpin axis.

When we consider the influence of the wheel normal force only (constant and the same for left and right wheel), the resulting torque at the kingpin axis (7) varies according to the parameter r_p only (6), what is shown in Fig. 5a for left and right wheel separately. In the range where the characteristic of r_p vs. δ_w (Fig. 4 left) has a positive slope, M_{ka} tends to self-align the steering system [1].

Left and right torque relative to the kingpin axis acts through the steering arm and the tie rod giving a steering rack force, what can be described by:

$$F_w = \frac{M_{ka,l}}{i_{pw,l}} - \frac{M_{ka,r}}{i_{pw,r}} \tag{8}$$

The resultant force at the steering rack is balanced in the design position ($p = 0$ and $\delta_h = 0$) for a symmetric steering system and load conditions, Fig. 5c.

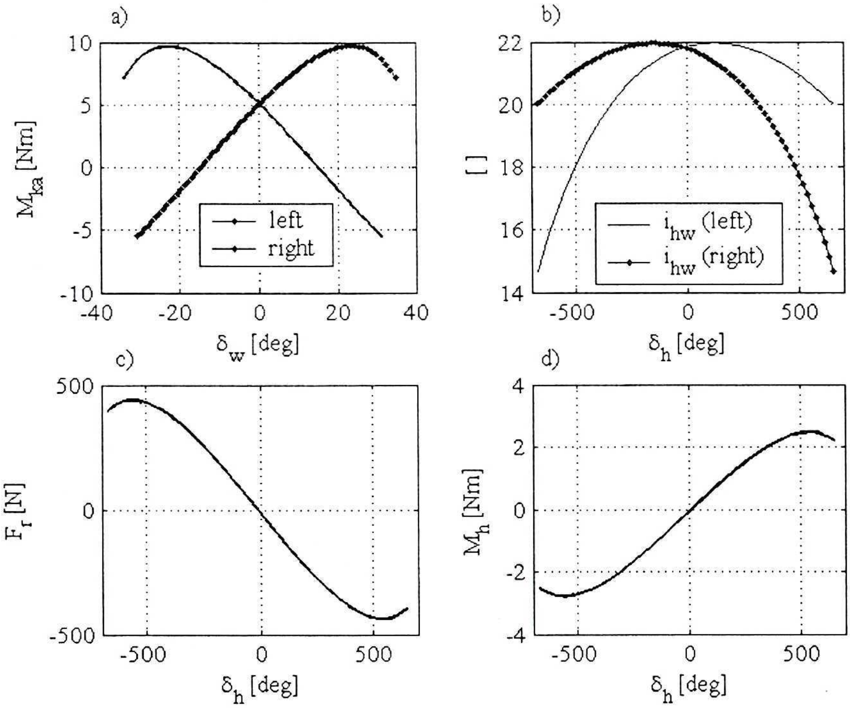

Fig. 5. Quasi-static characteristics of load transmission from the road wheels to the steering wheel resulting from the wheel normal force only (friction neglected): a) torque with respect to the kingpin axes versus steer angle, b) the overall kinematical ratio of steering system for left and right wheels, c) the steering rack force, d) torque at the steering wheel versus angle of steering wheel

Ultimately, the resistance torque that the driver has to exert in order to perform some maneuver is a function of both torques at the kingpin axis (Fig.5a) and the overall steering ratio described by equation (4). This ratio varies according to the steering angle in the manner shown in Fig.5b. The resulting handwheel torque can be determined by:

$$M_h = \frac{M_{ka,l}}{i_{hw,l}} - \frac{M_{ka,r}}{i_{hw,r}} \tag{9}$$

The same result can be obtained by reducing the rack force (8) to the handwheel with the constant gear ratio (2) taken into account.

The handwheel torque (9) treated as a function of the steering angle, shown in Fig.5d, is quasi-linear with a positive slope in the middle range of the steering angle, what is the necessary condition to achieve self-returnablity of the steering system. This condition is not fulfilled for steering angles greater than ca ±500 deg, where, in the absence of other forces, the steering system will attempt to displace further and to take its extreme position.

The friction forces and torques, determined for a real mechanism, have to be taken into account also at each step of the described load reduction. Their influence on the presented characteristics in Fig. 5 could be manifested by hysteresis loops and a loss of the steering system self-returnability in a certain range of steering displacements.

Simplified model for analysis of resistance forces

The resistance forces in the steering system excited by sinusoidal changes of the steering wheel angle can be analyzed by using a model more simple than the previous one, under the imposed assumptions. The model shown in Fig. 6a is composed of three lumped masses constraint to rotate in depicted hubs only. An angular position of the first body is described by the steering angle δ_h. The inertial moment J_1 of the first body with respect to its axis represents reduced inertial moments of the handwheel and a part of the steering shaft. The handwheel with steering shaft is joined with the steering pinion by the torsional spring c_{ss}.

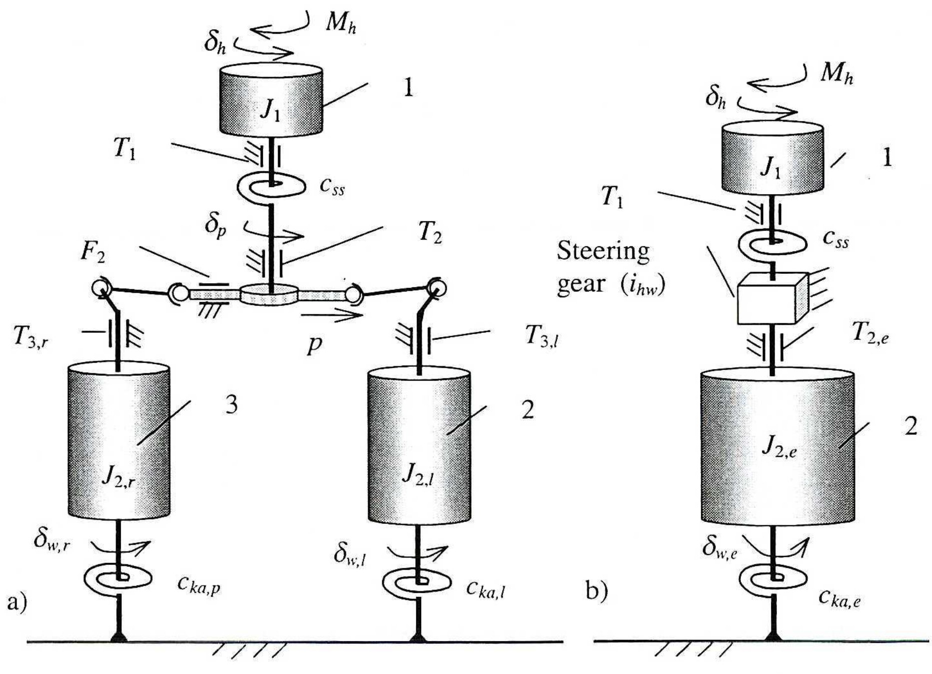

Fig. 6. The models of the steering system with: a) three lumped masses, b) two lumped masses valid for small amplitudes of steer angle changes

The car steering linkage with the rack-and-pinion transforms an angular displacement of the steering pinion δ_p into the rack displacement p, and next into the steer angular displacement of both road wheels, described by $\delta_{w,l}$ and $\delta_{w,r}$, and depicted in Fig. 6 as cylindrical bodies 2 and 3. Mass parameters of the road wheels, wheel knuckles, tie-rods, the steering rack and pinion are equivalently reduced to the kingpin axes, respectively for left (subscript – l) and right (subscript – r) wheels, yielding a compound moment of inertia J_2 for both sides respectively.

A body representing the road wheel with knuckle is joined with the base by torsional springs c_{ka} (left and right) that describe a conservative action of the wheel normal reaction force tending to self-align the steered wheel.

In Fig. 6a, the main places of friction in the system are also pointed out, where: T_1 represents the sum of friction torques in the steering shaft bearing and in two universal joints; T_2 corresponds to looses in the pinion bearing and friction in mesh, F_2 represents the friction force at the rack guides and yoke; and T_3 is the consequence of friction in the steel ball joints at the wheel knuckle, damper column, and column head for both sides respectively.

Assuming that the steering linkage is composed of rigid links only, the considered model is described by 2 degrees of freedom, for example δ_h and δ_p, and the configuration coordinates δ_p, p, $\delta_{w,l}$, $\delta_{w,r}$ are dependent according to kinematic constraints.

If the performed analysis is limited to small steering displacements only, further simplifications can be applied to the model depicted in Fig. 6a. The steering linkage ratio (3) can be assumed constant and the steer angles of both wheels equal to an equivalent $\delta_{w,e}$. This makes it possible to reduce inertial moments $J_{2,r}$, and $J_{2,l}$ into the one equivalent moment of inertia $J_{2,e}$.

This idea is presented in Fig. 6b, where two masses are connected in series by torsional spring c_{ss} and a gear box representing the steering linkage of constant ratio. The model has two rotational degrees of freedom described by δ_h and $\delta_{w,e}$. Both hubs depicted in Fig. 6b are characterized by proper friction torques, where T_1 is the same as in the model according to Fig. 6a, $T_{2,e}$ is the result of reduction of T_2, F_2, $T_{3,r}$ and $T_{3,l}$ onto the common axis.

5. In-door experiments

Exemplary results of the measurements are shown as time-domain functions in Fig. 7 for two frequencies of the harmonic excitation. The spatial four-bar linkage propelled by DC-Motor (Fig. 2), applied for turning the steering wheel, provides a good approximation of sinusoidal excitation with constant amplitude over the considered range of frequencies (top of Fig. 7). Torque at the handwheel, necessary to produce this enforced motion, oscillates about 0 in the range from –2.2 to +2.2 [Nm], what is shown in the center of Fig. 7. Forces in both tie rods oscillate symmetrically with the mean value corresponding to a slight compression state.

The relationship between the two generalized coordinates of the model, depicted in Fig. 6b, was determined by using spectral analysis for the excitation type and conditions of experiments presented in the paper, taking the rate of the wheel steer angle as an input signal and the rate of the steering angle as an output. Exemplary results are presented in Fig. 8. The steering system was excited by a pseudo-sinusoidal changes of the steering wheel angle with continuously increasing frequency from 1 to 3 Hz and amplitude 25 deg .

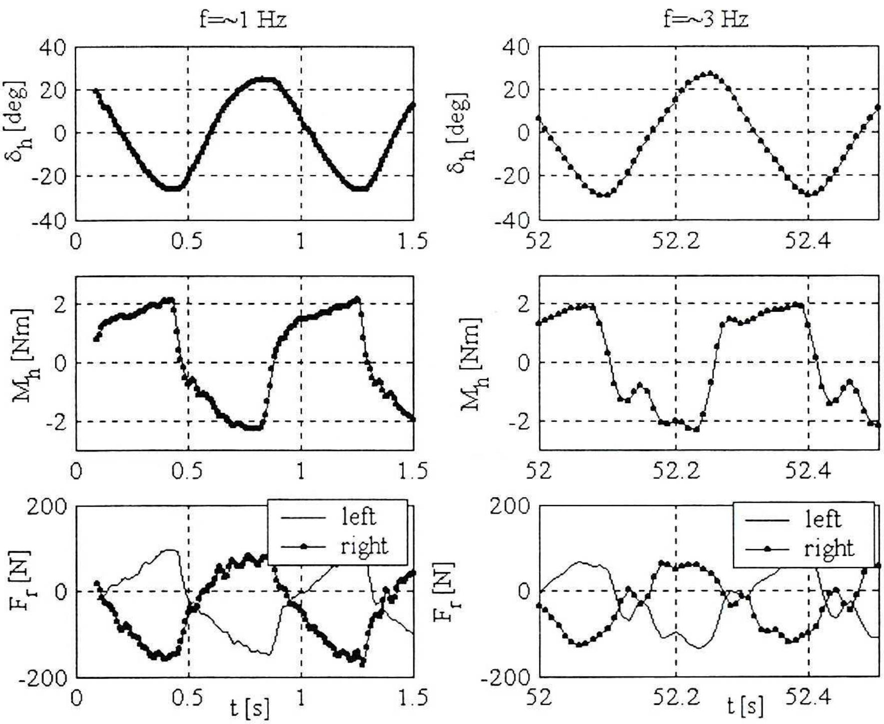

Fig. 7. Time responses of the steering system. Top: harmonic changes of the steering angle δ_h. Center: resistance torque at the handwheel M_h. Down: axial forces F_r in the tie rods. Frequency $f \approx 1$ Hz (a) and $f \approx 3$ Hz (b). Front wheels supported at the rotating plates

The high value of coherence function (top of Fig. 8) in the considered frequency interval justifies the use of spectral analysis. Satisfactory repeatability of the measurements is confirmed by fidelity of the presented results obtained in three repetitions, what can be noticed in Fig. 8 in the region where the coherence is close to 1. Out of this range the measurement uncertainty is high and the results can not be interpreted.

The module of Frequency Response Function (FRF) shown in the central part of Fig. 8 represents the dynamic overall ratio of the steering system. For the quasi-static excitation, when frequency is close to 0 in Fig. 8, its value corresponds to the one given by (1). Changes of the dynamic steering ratio in the considered range of frequencies are noticeable and reach about 10 %.

The argument of the FRF describes the phase shift between the input and output, bottom part of Fig. 8. This phase shift grows linearly by about 15 deg.

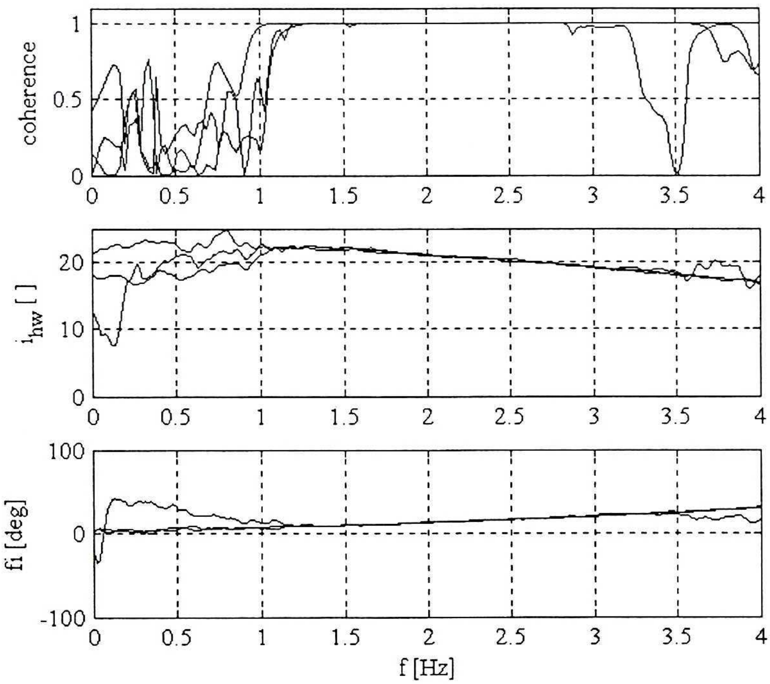

Fig. 8. Frequency domain relationships (coherence, module and phase shift) between input signal – rate of the wheel steer angle and output signal – rate of the steering angle for a pseudo-sinusoidal excitation with an amplitude of 25 deg. Front wheels supported at the rotating plates. Results of three trial repetitions are superimposed

On the basis of the determined FRF characteristics, we can estimate some parameters of the steering system model from Fig. 6b. The presented and other experimental results justify the assumption that the system fundamental frequency is above 10 Hz. Thus, some further simplifications for the model in Fig. 6b can be assumed, for example replacing the torsional spring c_{ss} by a rigid coupling of two masses (1 and 2) for the analysis in lower frequency band (up to 3 Hz) and with a limited torsional load in the steering system.

Estimation of the simplified model parameters

It is assumed that the steering torque measured at the handwheel, for load and excitation conditions considered here, can be described as the following function of the steering angle:

$$M_h = c_{h,e}\delta_h + J_{h,e}\ddot{\delta}_h \pm T_{h,e} \tag{10}$$

where:

$$c_{h,e} = \frac{c_{ka,e}}{i_{hw}^{\ 2}} \tag{11}$$

describes the equivalent stiffness (stabilization) coefficient of the steering system reduced to the handwheel,

$$J_{h,e} = J_1 + \frac{J_{2,e}}{i_{hw}^{\ 2}} \tag{12}$$

is the moment of inertia of the steering system reduced to the handwheel,

$$T_{h,e} = T_1 + \frac{T_{2,e}}{i_{hw}} \tag{13}$$

$T_{h,e}$ – friction torque of the steering system reduced to the handwheel.

Simultaneous measurement of forces in the tie rods makes it possible to separate different factors contributing to the resultant torque at the handwheel (10). Using the tie rods forces we can determine the reaction torque at the equivalent kingpin axis, below the steering gear box shown in Fig.6b, as a function of the wheel steer angle. This torque, in turn, should be equal to:

$$M_{ka} = c_{ka,e}\delta_{w,e} + J_{2,e}\ddot{\delta}_{w,e} \pm T_{2,e} \tag{14}$$

The time functions of the handwheel torque and steering wheel angle, presented in Fig. 7, can be used to determine parametric characteristics, shown in Fig. 9, describing the resistance torque at the handwheel (a) and the left tie rod force (b) vs. the steering angle.

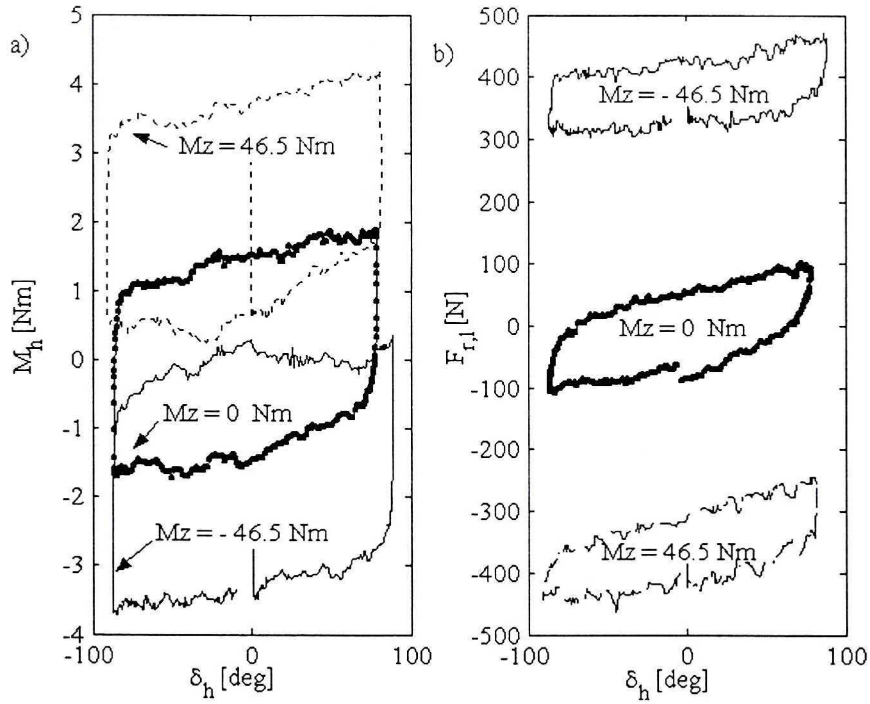

Fig. 9. a) The handwheel resistant torque and b) reaction force in the left tie rod versus the steering angle. Quasi-static sinusoidal excitation of the steering angle. The front wheels are supported at rotating plates, and the left one is loaded by a constant aligning torque M_z (with values: –46.5, 0, 46.5 [Nm]). Suspension in the design position

The characteristics presented in Fig. 9 are typical for a mechanical system with stiffness and friction. Slope of the characteristics (loops) dependents on the self-aligning torque caused by the normal reaction force exerted from the ground on the road wheel. Width of the loops represents equivalent friction moments or forces in the joints. Although the stabililization coefficient is positive under load conditions fixed for measurements, the friction forces cause that the steering system is not characterized by self-returnability in this range of steering angle displacements.

The same features can be noticed in both diagrams in Fig. 10, where case (a) is similar to Fig. 9a, and case (b) is the resistant torque M_{ka} relative to the kingpin axis, determined on the basis of the tie rod forces, Fig. 9b. The wheel steer angle δ_w is determined on the basis of the measured δ_h and the proper steering ratio (4).

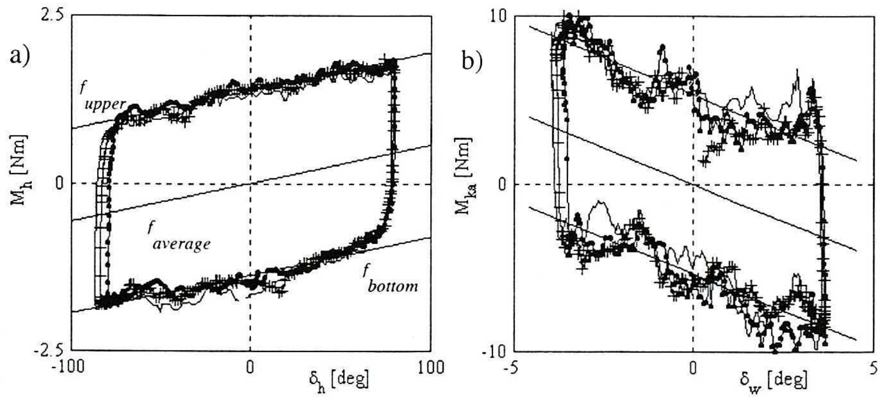

Fig. 10. Exemplary characteristics of a) steering torque vs. steering angle, and b) torque with respect to kingpin axis vs. left wheel steer angle for a sinusoidal steering angle excitation (f = 0.1 Hz). Front wheels supported at the rotating plates. Results of three trial repetitions are superimposed

Parameters used in equations (10) and (14), which describe the model in Fig. 6b, can be estimated on the basis of the introduced characteristics in the following way. Considering the measurement results of the handwheel torque and the steering angle excited in pseudo-sinusoidal manner, properly handled in order to obtain the characteristic in Fig. 10a, one can approximate its upper and bottom part separately by a linear function of δ_h in the form:

$$f(\delta_h) = k_1\delta_h + k_2 \tag{15}$$

where:

k_1 – slope parameter that includes stiffness and inertia effects,

k_2 – intercept parameter corresponding to equivalent moment of friction forces.

The same procedure applies to the characteristics in Fig. 10b of equivalent resistance torque at the kingpin axis versus the wheel steer angle.

The estimated parameters, obtained by averaging the linear function coefficients for upper and bottom parts of each characteristics shown in Fig. 10, determined experimentally on the basis of three repetitions, are the following:

$T_{h,e} = 1.37 \pm 0.05$ Nm; $c_{h,e} = 0.0057 \pm 0.0006$ Nm/deg; $T_{2,e} = 10.70 \pm 0.73$ Nm; $c_{ka,e} = 1.67 \pm 0.42$ Nm/deg.

Satisfactory repeatability of the measurement results is confirmed by fidelity of the presented results obtained in three repetitions superimposed in Fig. 10.

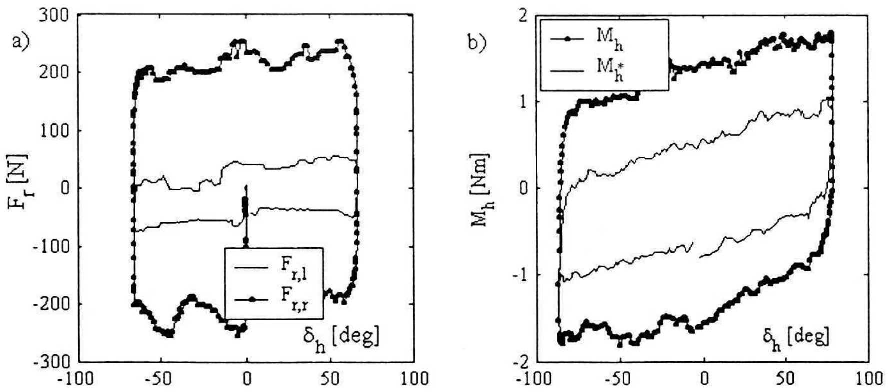

Fig. 11. a) The reaction forces in both tie rods versus the steering angle. Steering system with free rotating handwheel is moved from its initial position by exerting a moment of forces M_z at the right wheel. b) Comparison of the resistant torque M_h, measured at the handwheel, and M_h^* determined using formula (9). Suspension in the design position

6. Results and interpretation

Parameters of the formulated model were estimated on the basis of the experimental results, obtained for different load conditions (defined above) and frequencies of the pseudo-sinusoidal excitation, on the basis of the parametric characteristics of the form shown in Figs 9 and 10.

Fig. 9 presents the influence of the steering system load, changed by a constant moment of forces M_z, exerted at the rotating plate of the left wheel, on characteristics of the handwheel resistant torque (a) and reaction force in the left tie rod (b) versus the steering angle. Under the quasi-static sinusoidal excitation of the steering angle, and for described magnitudes of M_z (−46.5, 0.0, 46.5 [Nm]), the slope of the characteristics does not change significantly and the width of hysteresis loops changes very slightly.

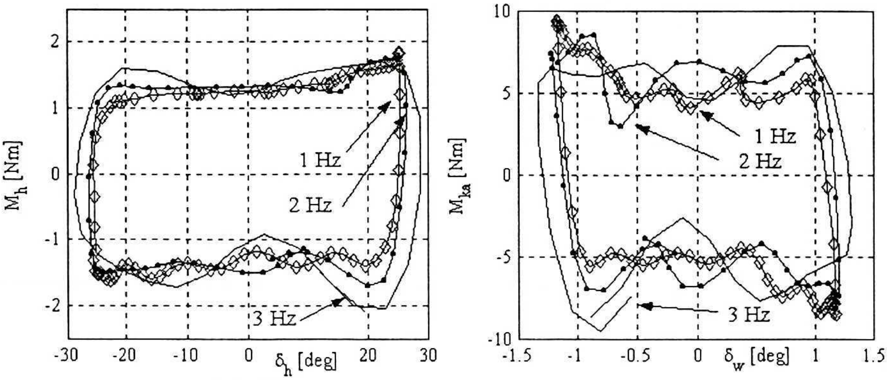

Fig. 12. Steering torque vs. steering angle (left), and torque relative to kingpin axis vs. left wheel steer angle (right) for a sinusoidal steering angle excitation with frequency f = 1, 2, and 3 Hz. Front wheels supported at the rotating plates, F_z^P = 2.50 kN

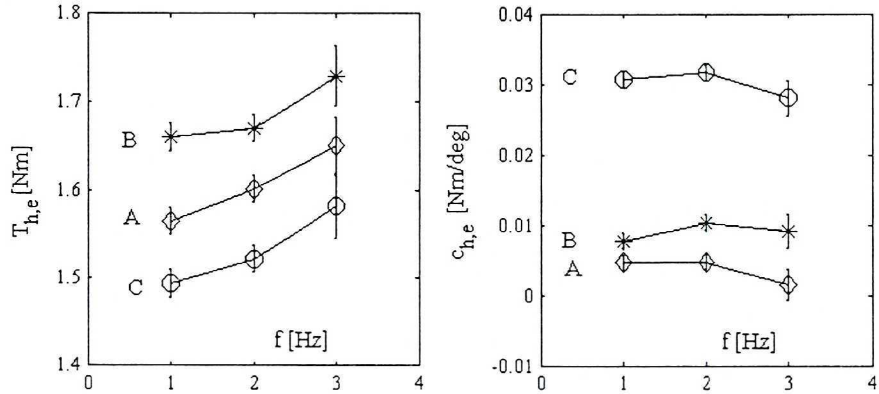

Fig. 13. Estimates of the model parameters reduced to the handwheel. Influence of the pseudo-sinusoidal excitation frequency and different load conditions (A, B, C) is presented

In order to distinguish different friction forces in the steering system, the following experimental trials were carried out. In the first trial the steering system, with a free rotating handwheel, is moved from its initial position by exerting a quasi-static moment of forces M_z at the rotating plate of the right wheel. The corresponding steer displacement of the right wheel is transferred by the right tie rod into displacements of the steering rack, pinion, steering shaft with the handwheel. Ultimately, the left wheel supported on a free rotating plate is steered symmetrically to the right side through the left tie rod. The functions of reaction forces in both tie rods versus the steering angle are presented in Fig. 11a. The slopes of the obtained characteristics are identical. The width of the hysteresis loop for the left tie rod is a consequence of a total friction torque with respect to the kingpin axis, resulting from steel ball joints, strut slider and rotating plate of the suspension left side. Difference in the friction force of about 160 N between the characteristics of right and left tie rod corresponds to the looses in the rack and pinion steering gear.

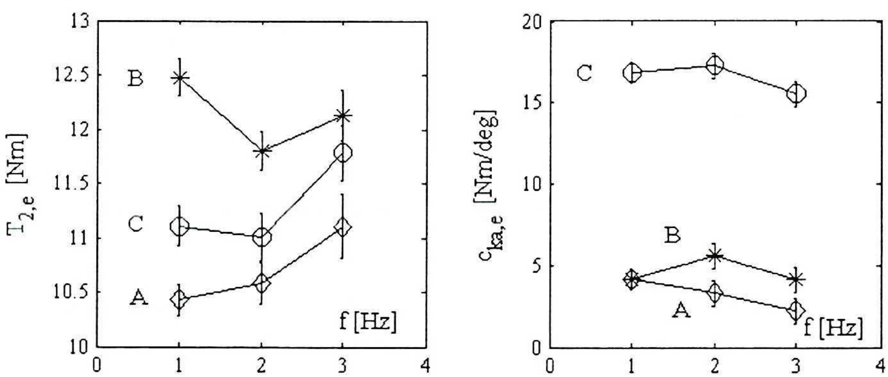

Fig. 14. Estimates of the model parameters reduced to the kingpin axis. Influence of the pseudo-sinusoidal excitation frequency and different load conditions (A, B, C) is presented

In Fig. 11-b, the resistant torque M_h measured at the handwheel is compared with M_h^* determined using formula (9) on the basis of resistant torques at kingpin axes, known from measurements of the respective tie rod forces. This trial conditions include quasi-static sinusoidal excitation of the steering angle, with the front wheels supported by free rotating plates. The slopes of the obtained characteristics are virtually the same. The difference in friction torque of about 0.7 Nm between the characteristics of M_h and M_h^* corresponds to the looses in the rack and pinion steering gear.

An influence of the excitation frequency of the steering wheel angular displacements on the steering system response is noticeable in Fig. 12, where characteristics similar to the ones in Fig. 10 are presented. The parameters of the formulated model (Fig. 6b) were estimated for each excitation frequency and different load conditions. Their mean values with confidence bounds are presented collectively in Figs 13 and 14. Changes of the excitation frequency and load conditions involve only minor alteration of the obtained estimates.

7. Conclusions

The presented results of the in-door experiments and the formulated model of the wheel guiding mechanism allow us to study stabilization and insensitivity characteristics of the car steering system. These specific properties are important in the aspects of driver comfort, effort, and feeling, and car directional stability, corresponding to the typical maneuvers at high speed of cruising but with small lateral acceleration. Under these operation conditions, the resistance torque at the handwheel, subjectively evaluated by the driver, is a consequence primarily of the wheel vertical forces and friction forces in joints of the suspension/steering mechanism.

The assumptions taken in the paper were validated on the basis of experimental results. The friction forces in the joints of the steering system were characterized by a lack of clear dependency on sense and rate of the relative displacement. Stiction coefficient was indistinguishable from sliding coefficient. Fundamental frequency of the suspension-steering system was over 10 Hz. Inertial properties of the steering system and torsional compliance of the steering shaft had a negligible influence on resistance torque at the steering wheel under excitation and load conditions considered in the paper.

Resultant friction torque at the handwheel is primarily influenced by the friction in the steering rack guides (about 50%) and friction forces in the ball joints (about 50%) in the steering linkage. Due to a preload of the ball joints, applied in the assembly process, and a preload of the yoke to the rack realized by a spring, the total friction torque is only slightly dependent on variations of the load in the steering system. The change of the excitation frequency involves only minor alteration of estimates of the model parameters.

The formulated model provides a basis for understanding the measurement results and for predicting the results of possible design and operating changes.

This research was supported by Grant No 8 T12C 061 20 founded by Polish Commitee of Science.

Manuscript received by Editorial Board, April 28, 2004;
final version, July 23, 2004.

REFERENCES

[1] Matschinsky W.: Radfuhrungen der Strassenfahrzeuge. Kinematik, Elasto-kinematik und Konstruktion. Springer-Verlag Berlin Heidelberg 1998.
[2] Morecki A., Knapczyk J., Kędzior K.: *Teoria mechanizmów i manipulatorów*. WNT Warszawa 2002.
[3] Neureder U.: Investigation into steering wheel nibble. Proc. Inst. Mech. Engrs, Vol. 216, Part D, 2002, pp. 267÷276.
[4] Sharp R.S., Granger R.: On car steering torques at parking speeds. Proc. Inst. Mech. Engrs, Vol. 217, Part D, 2003, pp. 87÷95.
[5] Stoll H.: Fahrwektechnik: Lenkanlagen und Hilfskraftlenkungen. Vogel Buchverlag, Wurzburg 1992.
[6] Wohnaas A.T.: Simulation von Kraftfahrzeug-Lenkungen unter besonderer Berucksichtigung von Reibung und Spiel. Dokt. Diss., Univ. Stuttgart 1994.

Badania stanowiskowe oporów w układzie kierowniczym samochodu osobowego z przekładnią zębatkową

Streszczenie

Przedstawiono wyniki badań oporów ruchu w układzie kierowniczym samochodu osobowego, uzyskane na stanowisku pomiarowym. Określono wpływ częstotliwości wymuszenia (w zakresie do 3 Hz) i zmian obciążenia na współczynnik stabilizacji i nieczułości układu kierowniczego z przekładnią zębatkową bez urządzenia wspomagającego. Analizowane charakterystyki opisano w postaci modelu zbudowanego z elementów sprężystych, inercyjnych i tarcia Coulomba. Porównano estymaty parametrów modelu (momentu sił tarcia i współczynnika sztywności) uzyskane w różnych warunkach badań.